CHAPTER III

The Use of Hydroponics Gel as a New Electrolyte Gelling Agent for Alkaline Zinc-Air Cell

3.1 Introduction

The zinc-air electrochemical power source possesses the highest energy density compared to other zinc anode batteries. This is mainly due to the unlimited and free supply of oxygen from the ambient air that is not incorporated within the cell. As the air electrode must be sufficiently porous to permit the air passage, the zinc-air battery is susceptible to water loss and hence the electrolyte drying out especially at elevated working temperatures. Lead-acid batteries share the common problem of the electrolyte drying out due to overcharging. The gelling of the lead acid battery electrolyte not only minimizes the water loss, furthermore it enhances the performance of the battery [*Dietz et. al, 1985; Vinod and Vijayamohanan, 1994; Vinod and Vijayamohanan, 2000; Vinod et. al, 1998*].

In view of these favorable benefits, especially the capability of the gelled electrolyte to minimize its water loss, the present work is initiated with the application of gelled electrolyte for use in alkaline zinc-air cells. The gelled electrolyte consists of elastic jelly granules obtained from hydroponics gel. Hydroponics gel is a medium used to store water and soluble nutrients in hydroponics technology where plants are grown in nutrient-rich water rather than soil. Hydroponics gel is attractive due to its ability to store solutions from 20 up to 100 times its weight, depending on types. This minimizes the weight of the cell. Upon mixture with solution, the gel expands into loosely bound elastic jelly granules and thus reduces the amount of electrolyte that is required to occupy a particular cell volume. Compared to other gelling agent commonly used,

cellulose or cellulose derivatives such as carboxymethylcellulose (CMC) [*Appelt and Malanowski, 1979; Cahoon and Holand, 1971; Morehouse et al, 1961*], vinyl polymers such as polyvinyl alcohol (PVA) [*Huot, 1997; Naylor, 1995*], and polytetrafluoroethlyne (PTFE) [*Ikeya, 1993; Vassal et. al, 1999*], hydroponics gel is cheaper. Further, there is a certain limit where the polymer-type material tends to shield and reduce the capacity of the cells [*Huot, 1997*], whereas hydroponics gel merely absorbs and stores the electrolyte.

3.2 Experimental

3.2.1 Cell components, design and fabrication

The zinc-air cell comprised a zinc anode, a caustic alkali electrolyte, and a carbon-based electrode sheet. All components were enclosed in a home-made cylindrical plastic casing of dimensions 28-mm in height and 45-mm in diameter. Both ends were attached with screwed, L-shaped, plastic rings. The container and both rings weighed 12.8 g.

A 0.4-mm thick zinc foil of 99.98 % purity was cut into a circular anode plate 45-mm in diameter. A current tab of copper foil (5 mm x 7 mm x 0.1 mm) was soldered to the centre of the plate. The zinc plate was first cleaned with acetone to remove any traces of oil or grease. Then it was dipped in 10% nitric acid solution for several seconds to remove the oxide and carbonate layers. Finally, it was air dried, weighed and stored in a desiccator. The circular zinc plate with a copper current tab weighed 4.6 g.

A commercially available, carbon-based, air cathode sheet was utilized. This consisted of laminated structures of fibrous carbon blended with a manganese catalyst and PTFE binder, supported by a nickel mesh that also acted as the current-collector. The air-side of the electrode was coated with a gas permeable, hydrophobic, Teflon layer. The whole structure was approximately 0.6 mm thick. Similarly, the air cathode sheet was cut into a 45-mm diameter circular shape with a small portion left for the cathode current tab. The air electrode with the current tab weighed 0.95 g. A cross-sectional view of the air cathode is shown schematically in Figure 3.1a. The electron micrographs in Figures 3.1 b and 3.1c give a closer observation on the fibrous carbon structure.

A comparatively low concentration of aqueous potassium hydroxide solution was used (2.8 M) [*Bagotzky and Skundin, 1980*] and hydroponics gel was introduced as an electrolyte-immobilizing agent. The gel was initially in granular form. On mixing with the aqueous potassium hydroxide solution, the gel expanded into loosely bound, elastic, jelly granules. 2.18 g of the gel was sufficient to contain 37 ml of potassium hydroxide solution that is 17 times its weight, and filled the 45-cm^3 casing volume, which corresponds to a 22 % volume expansion.

The construction of the components into a complete cell of monopolar design is shown schematically in Figure 3.2. The electrodes were placed snugly onto the L-shape rings. First, the ring with the air cathode was attached to the container. The gelled electrolyte was then introduced. Finally, the container was encapsulated with the zinc anode ring. The interfaces between the components

were sealed with an epoxy resin adhesive to prevent electrolyte leakage. The epoxy resin adhesive is known to be resistant to caustic alkali electrolyte attack. The completely fabricated cell weighed 63 g.

3.2.2 Zinc-air cell characterization

The cells were characterized according to their open circuit voltage (OCV), voltage-current and power density curves, and discharge profiles at constant current. The cell was stored for 24 hours prior to discharge test. Discharge currents were 5, 50 and 100 mA, respectively. A BAS LG-50 Galvanostat electroanalytical system was used to perform the experiments.

3.2.3 Electrode Characterization

X-ray Diffraction (XRD) measurements were undertaken on both the zinc anode and the air cathode before assembly in the cell. This involved the use of a Philips X-Ray Diffractometer XD-5 with Cu-K_α radiation (1.5405 Å). After the cells were fully discharged, they were dismantled, cleaned and air-dried. XRD measurements were again performed onto the electrodes. The latter measurements were taken to determine the failure mode of the fabricated cells. Scanning electron micrographs (SEM) were also taken to support the XRD observations.

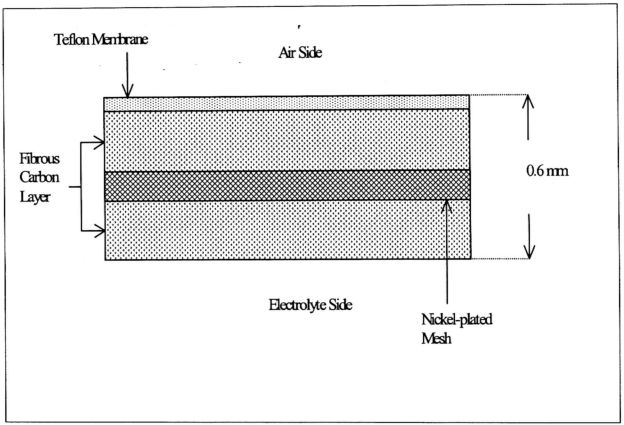

Figure 3.1(a). Schematic cross-sectional view of the air cathode used.

Figure 3.1 (b). Electron micrograph showing the fibrous carbon structure of the air electrode.

Figure 3.1 (c). The fibrous carbon structure at higher magnification.

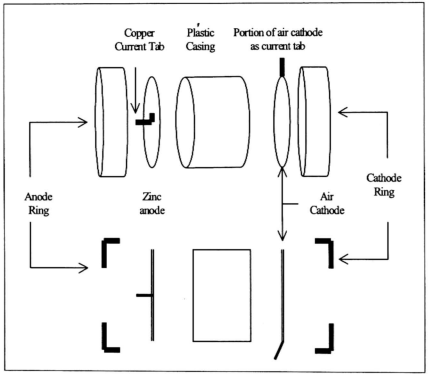

Figure 3.2. Schematic layout of the zinc-air cell assembly.

3.3 Results

3.3.1 Cell characterization

The open circuit voltage (OCV) values of the cells were 1.45 ± 0.5 V. The OCV remained stable, without any significant drop, during 24 hours of storage (see Figure 3.3). The operating voltage and the power density delivered by the cell as a function of current drain from 10.0 μA to 100.0 mA are given in Figure 3.4. The measurements were conducted after 24 hours of storage. The cell voltage at each particular current drain was monitored for 10 s and the average value was recorded. The power of the cell was calculated from the measured voltage-current curve.

Discharge profiles at constant currents of 100 and 50 mA are given in Figure 3.5 and the profile at a constant current of 5 mA in Figure 3.6. The cells are able to sustain the current drains, as demonstrated from the flat discharge curves. The average operating voltage was 1.08, 1.15 and 1.28 V, respectively. The cutoff voltage was around 0.9 V. At a current drain of 100 mA, the discharge lasted for 69 minutes, i.e. the time interval from the beginning of discharge to the cutoff voltage. At 50.0 and 5.0 mA, the discharge was sustained for 198 and 2750 min (45.8 hours), respectively.

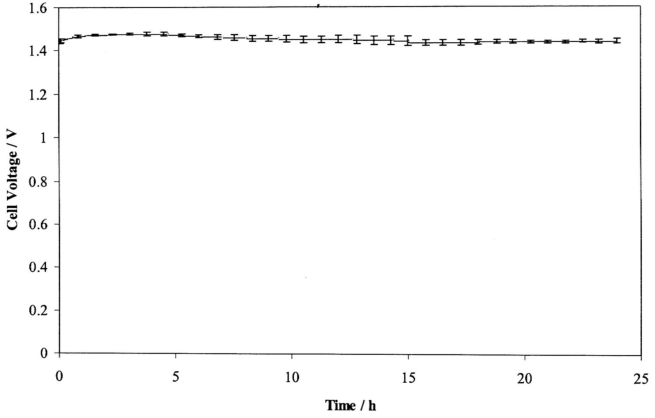

Figure 3.3. Zinc-air cell open circuit potential during 24 hours of storage

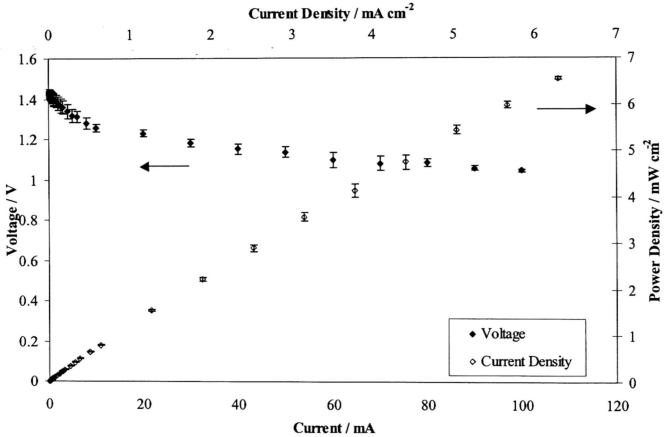

Figure 3.4. Zinc-air cell operating voltage and power density profiles as a function of discharge current.

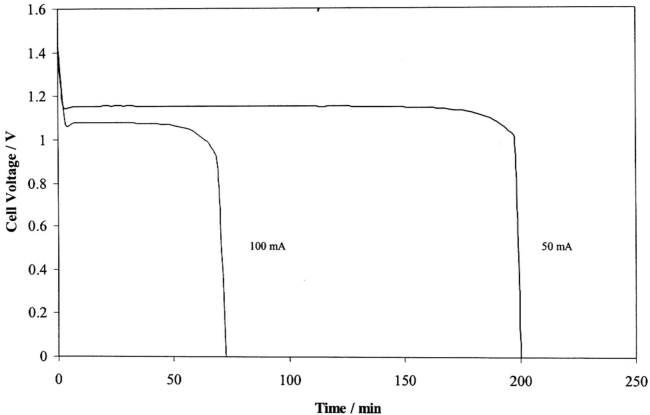

Figure 3.5. Discharge profiles at constant current of 100 and 50 mA.

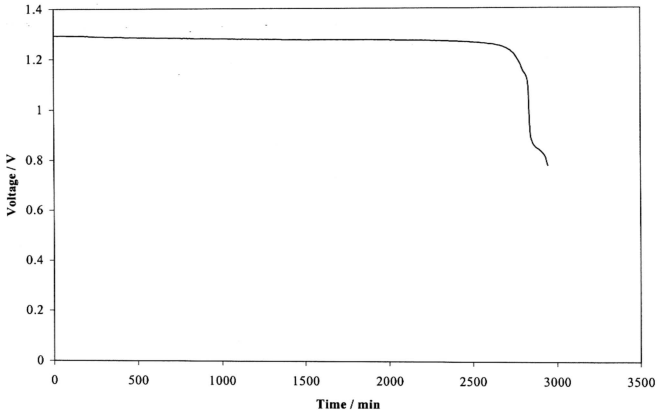

Figure 3.6. Discharge curve at constant current of 5 mA

3.3.2 Electrode characterization

The XRD pattern of the zinc plate before use is shown in Figure 3.7. It conforms to the standard ASTM X-ray data file pattern of zinc [*ASTM 4-0831, 1967*]. The XRD patterns of the post discharge zinc plates (Figure 3.8) was that for zinc oxide [*Izaki and Omi, 1997; ASTM 5-0664, 1967*], which is taken to be the end-product of the discharge. The XRD pattern of the air cathode before use is given in Figure 3.9. Three peaks are detected at 2θ angles of 18.2°, 44.6° and 52°. Later, the fibrous carbon layers were separated from the nickel-plated mesh, and XRD measurements were performed on each material (see Figures 3.10 and 3.11, respectively). Therefore, from the peaks detected in Figure 3.9, the 18.2° peak is attributed to the fibrous carbon material whereas the 44.6° and 52° peaks are assigned to the nickel-plated mesh. A comparison was made with the standard XRD pattern of nickel [*ASTM 4-0850, 1967*]. The 44.6° and 52° peaks match to the two strongest lines of the standard nickel XRD pattern. The XRD pattern of the air cathode after use remained unchanged.

The electron micrographs of the zinc anode before use is given in Figures 3.12a and 3.12b, showing the compact nature of the zinc plate. While the electron micrographs of the zinc plate taken after complete discharge showed that a long needle-like layer of zinc oxide layer covered the plate, as shown in Figures 3.13a to 3.13c at 1000, 5000 and 10000 magnifications, respectively. The above XRD results are in agreement with these observations.

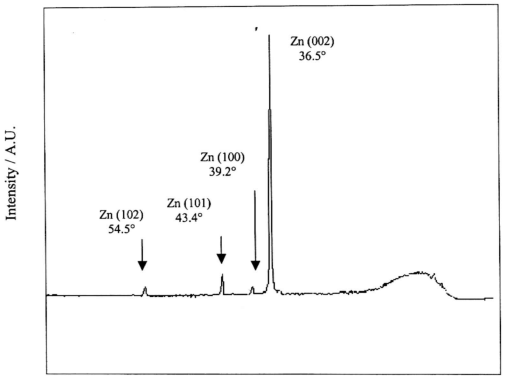

Figure 3.7. X-ray diffractogram of the zinc plate before use.

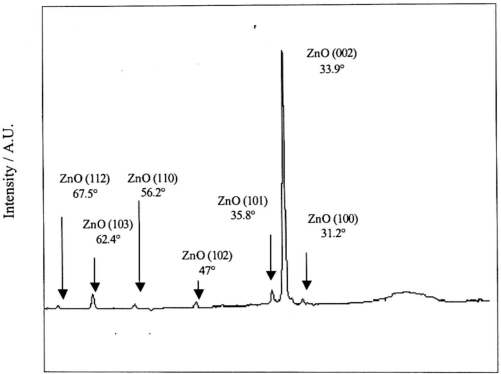

Figure 3.8. The X-ray diffractogram obtained from the zinc plate after complete discharge that matches to the zinc oxide pattern.

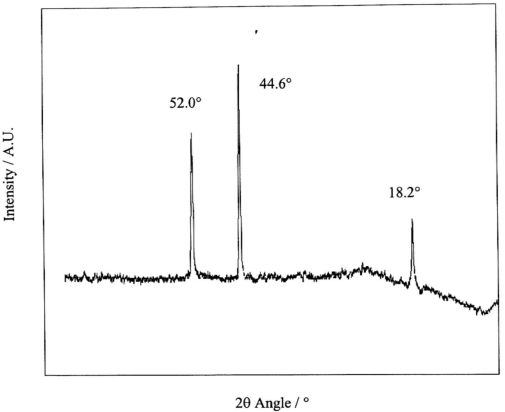

Figure 3.9. XRD pattern of the air cathode sheet. The sheet consists of fibrous carbon layers, nickel-plated mesh and Teflon membrane.

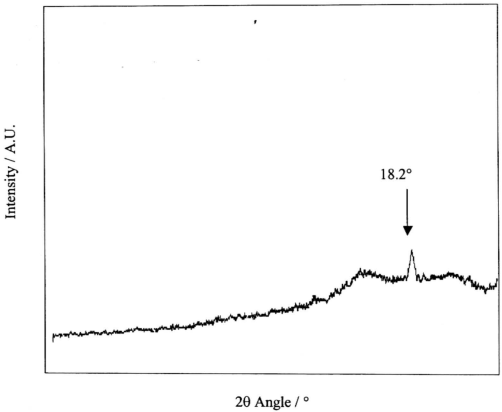

Figure 3.10. XRD pattern of the fibrous carbon layer of the air electrode sheet.

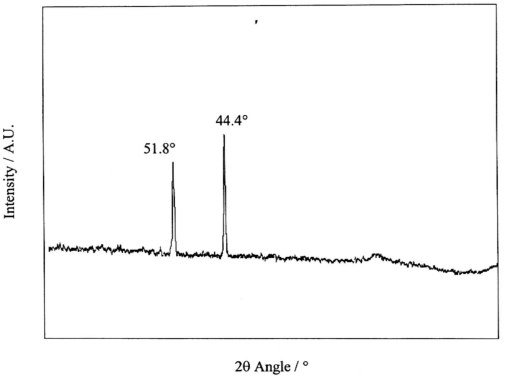

Figure 3.11. XRD pattern of nickel-plated mesh from the air electrode sheet.

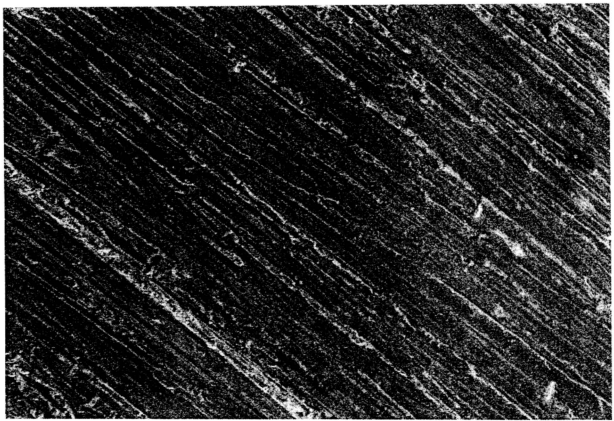

Figure 3.12 (a). SEM micrograph of the zinc plate before use at 600x magnification.

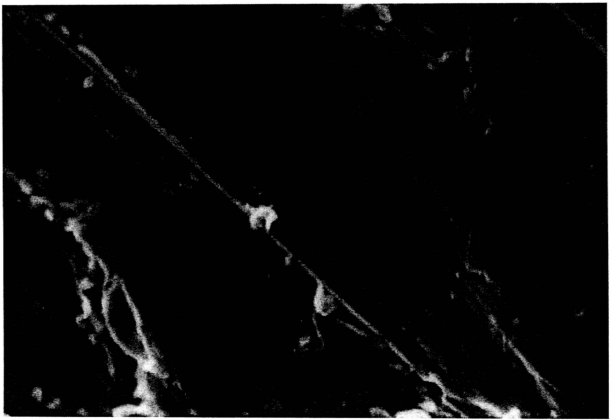

Figure 3.12 (b). SEM micrograph of the zinc plate before use at 10000x magnification.

Figure 3.13 (a). Scanning electron micrograph of the zinc anode plate after complete discharge displays the carpet-like zinc oxide layer.

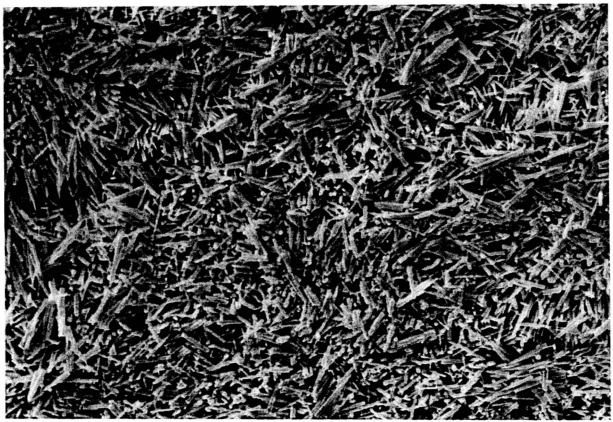

Figure 3.13 (b). Scanning electron micrograph of the zinc anode plate after discharge at higher magnification reveals the needle-like zinc oxide crystals.

Figure 3.13 (c). Zinc oxide needle-like crystal structures at 10000x magnification.

3.4 Discussion

Zinc-air cells have been fabricated employing a comparatively low concentration 2.8 M aqueous potassium hydroxide and hydroponics gel as the electrolyte gelling agent. OCV measurements over a period of 24 hours do not show any sign of fast self-discharge. The cell close-circuit operating voltage in the 10μA to 100 mA current range is in agreement with reported data, which is in the range 1.1-1.35 V [*Bender et. al, 1995; Crompton, 2000; Hamlen, 1995; Vincent et. al, 1984*]. The cells are capable of delivering 5, 50 and 100 mA constant current drains with resulting capacities of 229, 165 and 115 mAh, respectively. The use of hydroponics gel as an alkaline electrolyte gelling agent does not affect the oxidation-reduction reaction of the zinc-air cell, as is evident from the discharge capability of the cells. It should be noted that the resulting cell capacities are much lower than expected from the 4.5 g zinc electrode, which is 36900 mAh (4.5 g x 0.82 Ah g^{-1}). Presumably, this is because the electrode has a compact planar form. A zinc electrode in the massive or compact plate form cannot sustain a current as high as a powdered zinc anode [*Falk and Salkind, 1969*]. Further, the concentration of potassium hydroxide electrolyte was only 2.8 M. Normally, zinc-based batteries employ a potassium hydroxide concentration in the range 27 to 40 wt. % (6-10 M) [*Bagotzky and Skundin, 1980*]. Thus, the use of a highly porous and expanded zinc electrode, and potassium hydroxide of substantially higher concentration would definitely improve utilization of the zinc active material.

XRD results show that the failure of the cell at the end of discharge is due to the formation of an insulating layer of zinc oxide rather than any side reactions of the hydroponics gel with the zinc or the electrolyte. Electron micrographs show that a long needle-like layer of zinc oxide crystals is formed on the electrode. This supports the XRD observations.

3.5 Summary

Hydroponics gel is a promising alternative electrolyte gelling agent for zinc batteries and very likely for other alkaline electrolyte batteries such as nickel metal hydride. Primary, monopolar, zinc-air cells employing hydroponics gel as the electrolyte immobilizing agent have been fabricated and found to be capable of sustaining discharge loads of 5, 50 and 100 mA with corresponding capacities of 229, 165 and 115 mAh, respectively. The discharge capability of the cells and XRD analysis show that the inclusion of hydroponics gel into the aqueous potassium hydroxide electrolyte does not affect the electrochemistry of the zinc-air cell.

References

Appelt, K. and Malanowski, L., "A cylindrical R-20 size zinc-air primary cell", J. Power Sources 4 (**1979**) 91-95

ASTM X-Ray Powder Data File, J.V. Smith (Editor), Inorganic Vol., American Society for Testing and Materials (ASTM) (**1967**) 4-0831

ASTM X-Ray Powder Data File, J.V. Smith (Editor), Inorganic Vol., American Society for Testing and Materials (ASTM) (**1967**) 5-0664

Bagotzky, V.S. and Skundin, A.M., Chemical Power Sources, Academic Press (**1980**) Chap. 12

Bender, S.F., Cretzmeyer, J.W. and Reise, T.F., "Zinc/air cells", in: Handbook of Batteries, Linden, D., (Editor), McGraw-Hill Inc., 2nd Ed. (**1995**) pg. 13.3-13.19

Cahoon, N.C. and Holland, H.W., "The alkaline manganese dioxide:zinc system", in: The Primary Battery (Vol. 1), Heise, G.W. and Cahoon, N.C. (Editors), Wiley, New York (**1971**) pg. 239-262

Crompton, T.R., "Battery Reference Book", Newnes, 3rd Ed. (**2000**) pg. 26/3

Dietz, H., Garche, J. and Wiesner, K., "The effect of additives on the positive lead-acid battery electrode", J. Power Sources 14 (**1985**) 305-319

Falk, S.U. and Salkind, A.J., Alkaline Storage Batteries, John Wiley and Sons Inc. (**1969**) Chap. 3

Hamlen, R.P., "Metal/air batteries", in: Handbook of Batteries, Linden, D. (Editor), McGraw-Hill Inc., 2nd Ed., **1995**, pg. 38.1-38.45

Huot, J-Y, "Advances in zinc batteries", in: New Materials for Fuel Cell and Modern Battery Systems, Proceedings of the 2nd International Symposium on New Materials for Fuel Cell and Modern Battery Systems, Savadogo, O. and

Roberge, P.R. (Editors), Ecole Polytechnique de Montreal (Pub.) (**1997**) pg. 137-165

Ikeya, T., Kumai, K. and Iwahori, T., "Mechanical process for enhancing metal hydride for the anode of an Ni-MH secondary battery", J. Electrochem. Soc. 140 (**1993**) 3082-3086

Izaki, M. and Omi, T., "Characterization of transparent zinc oxide films prepared by electrochemical reaction", J. Electrochem. Soc., 144 (**1997**) 1949-1952

Morehouse, C.K., Glicksman, R. and Lozier, G.S., "Batteries", in: New Techniques for Energy Conversion, Levine, S.N. (Editor), Dover Pub. Inc., New York, **1961**, pg. 358-379

Naylor, D., "Mercuric oxide cells", in: Handbook of Batteries, Linden, D. (Editor), McGraw-Hill Inc., 2nd Ed. (**1995**) pg. 11.1-11.22

Vassal, N., Salmon, E. and Fauvarque, J-F., "Nickel/metal hydride secondary batteries using an alkaline solid polymer electrolyte", J. Electrochem. Soc. 146 (**1999**) 20-26

Vincent, C.A., Bonino, F., Lazzari, M. and Scrosati, B., Modern Batteries. An Introduction to Electrochemical Power Sources, Edward Arnold (Pub.) Ltd. (**1984**) pg. 90

Vinod, M.P. and Vijayamohanan, K., "Effect of gelling on the open circuit potential against time transients of $Pb/PbSO_4$ electrodes at various states of charge", J. Appl. Electrrochem. 24 (**1994**) 44-51

Vinod, M.P. and Vijayamohanan, K., "Effect of gelling on the impedance parameters of $Pb/PbSO_4$ electrode in maintenance-free lead acid batteries", J. Power Sources 89 (**2000**) 88-92

Vinod, M.P., Vijayamohanan, K. and Joshi, S., "Effect of silicate and phosphate additives on the kinetics of the oxygen evolution in valve-regulated lead/acid batteries", J. Power Sources 70 (**1998**) 103-105